



Cite this: *Chem. Sci.*, 2024, **15**, 18881

All publication charges for this article have been paid for by the Royal Society of Chemistry

## Adaptive photoluminescence through a bioinspired antioxidative mechanism†

Tobias Rex,<sup>ab</sup> Sebastian Baumert,<sup>c</sup> Alexander Hepp,<sup>Id</sup><sup>a</sup> Gustavo Fernández<sup>Id</sup><sup>\*c</sup> and Cristian A. Strassert<sup>Id</sup><sup>\*ab</sup>

Transition metal complexes are archetypal luminescent probes that are widely used for various applications ranging from optoelectronics to biomedicine. However, they face significant challenges such as photobleaching and photooxidative stress, which limit their performance. Herein, we introduce a photosystem-inspired concept based on the use of a vitamin (ascorbic acid, Asc-Ac) to adaptively suppress photobleaching of molecular luminophores. As a proof-of-concept compound, we have selected a new bis-cyclometalated Pt(II) complex (Pt-tBu) and investigated its adaptive photoluminescence resulting from singlet dioxygen ( $^1\text{O}_2$ ) photoproduction in the presence of Asc-Ac. Interestingly, the excited state quenching and subsequent photobleaching of Pt-tBu in aerated solutions is suppressed by addition of Asc-Ac, which scavenges the  $^1\text{O}_2$  photosensitized by Pt-tBu upon irradiation and results in an adaptive oxygen depletion with enhancement of luminescence. The adaptation is resilient for successive irradiation cycles with oxygen replenishment, until peroxidation overshooting leads to the degradation of Pt-tBu by formation of a dark Pt(IV) species. The complexity-related adaptation with initial overperformance (luminescence boost) relies on the external energy input and cascaded feedback loops, thus biomimicking inflammation, as the repeated exposure to a stressor leads to a final breakdown. Our antioxidative protection mechanism against photobleaching can be successfully extended to multiple coordination compounds (e.g., Ir(III), Ru(II) and Re(I) complexes), thus demonstrating its generality. Our findings broaden the scope of molecular adaptation and pave the way for enhancing the stability of molecular luminophores for multiple applications.

Received 9th September 2024

Accepted 9th October 2024

DOI: 10.1039/d4sc06096b

rsc.li/chemical-science

## Introduction

Biological systems employ diverse protective mechanisms to counteract degradation processes. A notable example is found in photosynthetic organisms,<sup>1</sup> where the generation of singlet dioxygen ( $^1\text{O}_2$ ) upon light irradiation with subsequent formation of triplet chlorophyll may lead to structural damage. To mitigate this threat, chloroplasts make use of defense mechanisms that involve scavenging of  $^1\text{O}_2$  by antioxidants such as  $\beta$ -carotene and  $\alpha$ -tocopherol.<sup>1</sup> Another prominent antioxidant is ascorbic acid (Asc-Ac; vitamin C), which neutralizes  $^1\text{O}_2$  to produce dehydroascorbate and  $\text{H}_2\text{O}_2$ , further illustrating the role of natural antioxidants in protecting cells from oxidative stress.<sup>2–5</sup> While such antioxidative mechanisms are

commonplace in biological systems, their role in artificial counterparts remains elusive.

A long-standing challenge in chemical systems that would greatly benefit from protective measures is the phenomenon of photobleaching.<sup>6</sup> Akin to biological systems, molecular luminophores are significantly affected by oxidative stress, which can modulate their properties and function.<sup>7–9</sup> Despite their widespread interest and versatile applications in optoelectronics,<sup>10–14</sup> bioimaging<sup>15–18</sup> and photocatalysis,<sup>19</sup> transition metal complexes (including Ru(II), Ir(III) and Pt(II) coordination compounds) are among the luminophores that suffer from photobleaching mainly due to Dexter energy transfer to triplet dioxygen, *i.e.*, quenching by  $^3\text{O}_2$  to yield highly reactive  $^1\text{O}_2$ .<sup>20–23</sup> As a result, they can be used as photosensitizers (PS)<sup>24–26</sup> in photodynamic therapy (PDT).<sup>27,28</sup> A prominent molecular design strategy to improve the performance and stability of Pt(II) complexes lies in the use of tetradeinate bis-cyclometallated ligands, which enable a stabilizing rigidification of the coordination environment.<sup>29–31</sup> However, if quenching is not suppressed by deoxygenation, photooxidative stress triggered by irradiation with  $^1\text{O}_2$  generation ultimately leads to degradation.<sup>32–34</sup> In recent years, various strategies have been developed to improve photostability through molecular

<sup>a</sup>Universität Münster, Institut für Anorganische und Analytische Chemie, Corrensstraße 28/30, 48149 Münster, Germany. E-mail: ca.s@uni-muenster.de

<sup>b</sup>Universität Münster, CeNTech, CiMIC, SoN, Heisenbergstraße 11, 48149 Münster, Germany

<sup>c</sup>Universität Münster, Organisch-Chemisches Institut, Corrensstraße 36, 48149 Münster, Germany. E-mail: fernand@uni-muenster.de

† Electronic supplementary information (ESI) available. See DOI: <https://doi.org/10.1039/d4sc06096b>



design.<sup>35</sup> These approaches include increasing the oxidation potential of molecules,<sup>36</sup> introducing structural changes in the auxiliary ligand<sup>37</sup> and creating supramolecular architectures such as micelles<sup>38</sup> to enhance photostability. Additionally, the linking of protective agents<sup>39</sup> or the embedding of lumophores in frameworks<sup>40,41</sup> as well as the use of chelate complexes<sup>42</sup> are effective methods for protection against chemical degradation. However, these strategies often alter the emission properties and the chemical environment of the luminophores. Therefore, there is a substantial need to develop alternative chemical approaches to stabilize luminophores in solution against oxidative stress while preserving their optical properties.

Herein, we introduce a bioinspired antioxidative strategy that adaptively suppresses quenching and prevents photo-bleaching of photosensitizing luminophores. To demonstrate our approach, we synthesized a Pt(II)-based luminophore bearing a tetradentate bis-cyclometalated ligand (**Pt-tBu**, Fig. 1)<sup>43,44</sup> and examined its adaptive response to irradiation in the presence of  $^3\text{O}_2$  and Asc-Ac (for synthesis and characterization, see Fig. S2†). The three peripheral *tert*-butyl groups of **Pt-tBu** were included to prevent aggregation, while the square-planar coordination geometry remains accessible to dioxygen. **Pt-tBu** exhibits an intense photoluminescence in liquid solutions upon deoxygenation, but it rapidly undergoes photo-bleaching if quenched by dissolved  $^3\text{O}_2$  (Fig. 1). Interestingly,

Asc-Ac scavenges the photosensitized  $^1\text{O}_2$  generated by **Pt-tBu**, leading to a significant luminescence enhancement due to the depletion of  $^3\text{O}_2$ . Re-equilibration with oxygen, followed by successive irradiation cycles, ultimately leads to the peroxidation of the **Pt-tBu** to a Pt(IV) species. Hence, the initial over-performance followed by breakdown upon repeated aggression resembles stress-adaptation of organisms leading to collapse, irreparable damage or chronic conditions, such as rheumatoid arthritis or other autoimmune diseases.<sup>45</sup>

## Results

The UV-vis absorption and photoluminescence spectra of **Pt-tBu** in organic solvents, such as dichloromethane (DCM) and dimethylformamide (DMF), show the characteristic photo-physical properties of Pt(II) complexes with tetradentate ligands (Table 1 and Fig. S34 and S35†).<sup>43</sup> The higher-energy absorption bands below 350 nm are attributed to transitions into  $^1\pi-\pi^*$  configurations, indicative of ligand-centered electronic states. Conversely, the lower-energy absorption bands appearing above 350 nm are associated with transitions into  $^1\text{LC}$  (ligand-centered) and  $^1\text{MLCT}$  (metal-to-ligand charge transfer) states. The photoluminescence spectra in DMF exhibit a maximum emission peaking at 514 nm, accompanied by a vibrational shoulder at 549 nm (metal-perturbed LC triplet state, *i.e.*,  $^3\text{MPLC}$ , Fig. 2b and S34†). The substantial differences in the

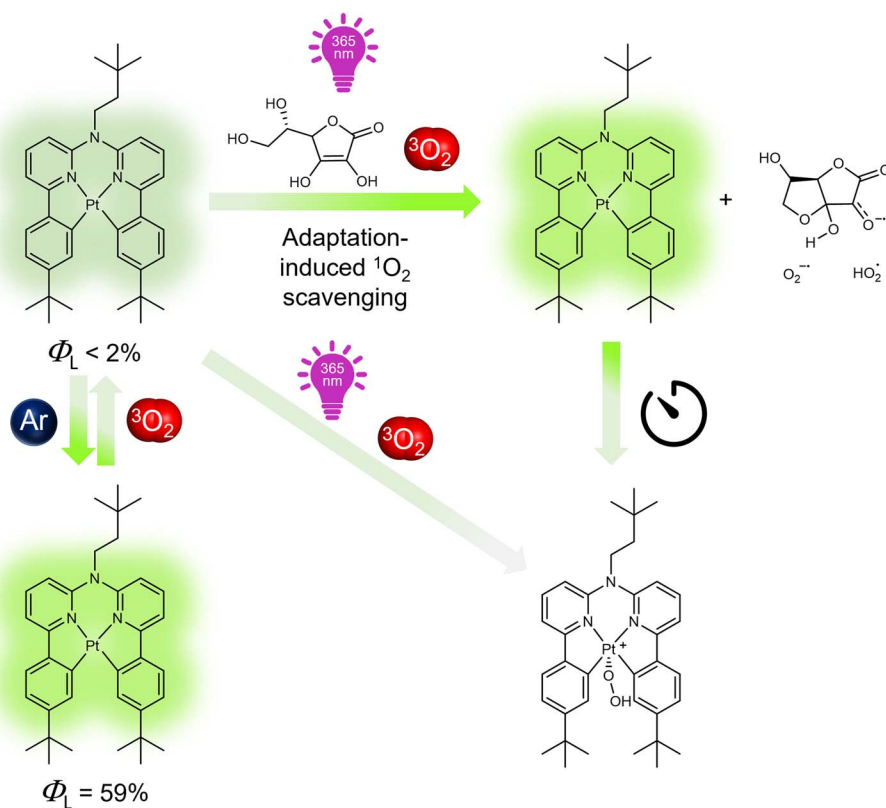


Fig. 1 Structural formula of **Pt-tBu** and schematic representation of its photoluminescence changes in response to light upon deoxygenation with Ar followed by equilibration with air, in the presence and absence of Asc-Ac. Feedback loops and light-driven equilibrium displacement enables the adaptation to the stressor ( $^3\text{O}_2$ ) through  $^1\text{O}_2$  scavenging.



Table 1 Summary of photophysical data for Pt-tBu

	$\Phi_{L(\text{air})} (\pm 2) (\%)$	$\Phi_{L(\text{Ar})} (\pm 3) (\%)$	$\tau_{(\text{air})} (\text{ns})$	$\tau_{(\text{Ar})} (\text{ns})$
Pt-tBu	<2	59	$124.6 \pm 0.3$	$6895 \pm 9$

quantum yields and excited state lifetimes observed before and after deoxygenation (Table 1) demonstrate the significant quenching effect by  $^3\text{O}_2$ .

The phosphorescence of **Pt-tBu** is quenched by  $^3\text{O}_2$  in a diffusion-controlled exciplex formation (Dexter energy transfer), leading to the production of  $^1\text{O}_2$ . In fact, the phosphorescence of  $^1\text{O}_2$  becomes evident in the NIR (peaking at 1275 nm, Fig. S37†).

To assess the potential degradation of **Pt-tBu** due to photo-oxidative stress, we examined its stability under UV irradiation ( $\lambda_{\text{ex}} = 365 \text{ nm}$ ) by measuring the UV-vis absorption spectra and the photoluminescence intensity (Fig. S35 and S36†). Subsequent irradiation of **Pt-tBu** solutions at two different concentrations (10  $\mu\text{M}$  and 25  $\mu\text{M}$ ) with UV light in a photoreactor revealed that **Pt-tBu** undergoes partial decomposition in the presence of  $^3\text{O}_2$ . This was verified by the loss of the  $^1\text{MLCT}$  band at 400 nm in the UV-vis spectra and the drop of emission intensity in the photoluminescence spectra (Fig. 2a, S35 and S36†). On the other hand, **Pt-tBu** exhibits resistance against UV irradiation upon deaeration, as evident from its invariant absorption and emission features (Fig. 2a, S38 and S39†). These results confirm that photosensitized  $^1\text{O}_2$  is the primary cause for the photobleaching of **Pt-tBu**.

To study the biomimetic protection involving an antioxidant, we prepared a mixture that combines Asc-Ac and **Pt-tBu**. In DMF, an excess of Asc-Ac in the presence of **Pt-tBu** under UV irradiation (in a photoreactor) indicated that the stressor ( $^3\text{O}_2$  photoconverted into  $^1\text{O}_2$ ) no longer affects the luminophoric PS **Pt-tBu**. Hence, only minor changes were observed in the MLCT absorption band before and directly after long-term irradiation (120 s, Fig. 2a and S40†).

The changes in the higher energy absorption bands (<400 nm) can be attributed to the formation of  $\text{H}_2\text{O}_2$ ,

dehydroascorbate, and a new coordination-chemical species (Fig. 1 and S40†). Furthermore, a narrowing of these bands becomes evident upon aging after irradiation (Fig S40,† right), which is accompanied by a decrease in the MLCT band located around 400 nm, which can be associated to the formation of a **Pt(iv)** species. Herein, a hydroperoxo ligand is incorporated upon oxidation of the former **Pt(ii)** complex, thus influencing both absorption and emission spectra. Remarkable, though, was the immediate boost of the emission intensity and the prolonged excited state lifetime of **Pt-tBu** (Fig. 2b and S49†).

To understand this behavior, we explored the influence of gradual irradiation on the emission intensity of **Pt-tBu** at two different concentrations (10  $\mu\text{M}$  and 25  $\mu\text{M}$ ), in order to double the  $^1\text{O}_2$  photoproduction rate, in the presence of Asc-Ac at two different concentrations (5 mM and 10 mM) (Fig. S41 and S42†). It was ensured that there was no gaseous headspace for the air-equilibrated system, as otherwise external oxygen could rediffuse into the solution. Notably, the phosphorescence intensities increased until they reached a plateau, indicating that the **Pt-tBu** is no longer quenched by  $^3\text{O}_2$  (Fig. 2c). In addition, we observed that both the concentration of **Pt-tBu** and the irradiation time (10 s and 15 s) influence the rate of adaptation. A higher concentration of **Pt-tBu** results in a reduced lag time to reach the plateau (Fig. 2c). We attribute this phenomenon to an increased  $^1\text{O}_2$  production rate and its trapping by the excess of Asc-Ac at higher concentrations of **Pt-tBu**. This suggests that  $^3\text{O}_2$  is converted to  $^1\text{O}_2$  and subsequently neutralized by Asc-Ac to form dehydroascorbate. In contrast, decreasing the irradiation intervals from 15 s to 10 s at a constant concentration (10  $\mu\text{M}$ ) resulted in a significantly delayed intensity rise (Fig. 2c). Thus, a substantial enhancement in emission can only be achieved upon extended irradiation (60 s). This can be explained by the slower oxygen photoactivation and reaction with Asc-Ac. On the other hand, we observed that an increase in the concentration of Asc-Ac from 5 mM to 10 mM had no effect on the onset. Note that the most efficient protection of the luminophore occurs using 200–1000 equivalents of ascorbic acid to ensure the quenching of the  $^1\text{O}_2$  produced during the irradiation process. Moreover, plotting  $(I/I_{\text{max}}) - 1$  vs. increasing quencher

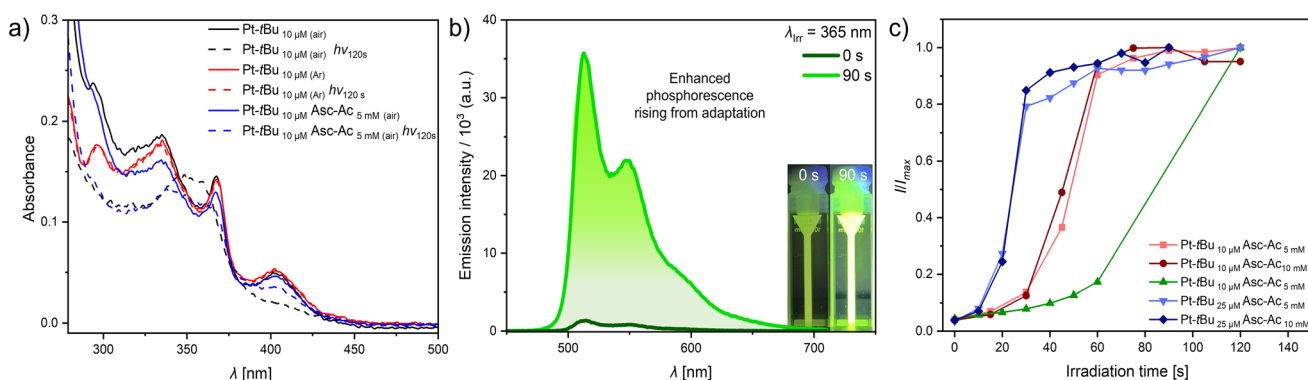


Fig. 2 (a) UV-vis absorption spectra of **Pt-tBu** in air-equilibrated DMF with (blue) and without (black) Asc-Ac, as well as of an Ar-purged (red) solution untreated (solid) and directly after irradiation (120 s) at 365 nm (dashed). (b) Exemplary photoluminescence spectra (**Pt-tBu** 10  $\mu\text{M}$  and Asc-Ac 5 mM) before and after prolonged irradiation in a photoreactor. Inset: pictures of the cuvette before and after the irradiation process in a photoreactor ( $\lambda_{\text{ex}} = 365 \text{ nm}$ ). (c) Plot of  $I/I_{\text{max}}$  vs. irradiation time at different concentrations of **Pt-tBu** and Asc-Ac at room temperature in DMF.



concentration (*i.e.*,  $vs.$   $1 - (t/t_{max})$ ), meaning progressively shorter irradiation times) revealed that the process can be represented in a Stern–Volmer-like plot (Fig. S43†). Besides the intensity changes, the lifetimes after reaching the plateau were measured. For **Pt-tBu** (10  $\mu$ M) with Asc-Ac (5 mM), the lifetime increased to  $\tau = 5.0$   $\mu$ s after irradiation (120 s). This contrasts with the shorter lifetime of  $\tau = 120$  ns observed for **Pt-tBu** in air-equilibrated solutions (Fig. S47 and S49†), confirming the partial scavenging of the quencher ( $^3\text{O}_2$ ). Nevertheless, it does not reach the lifetime upon full deoxygenation (*vide infra*), indicating the involvement of other quenching phenomena or residual  $^3\text{O}_2$ . This is also evidenced by the fluctuations within the plateau phase.

After a full irradiation cycle (90 s) of the sealed air-equilibrated mixture (identical to those in Fig. 2b) with a waiting period of one hour, the traces of re-diffused oxygen can be again scavenged, achieving the previous plateau yet without substantial photobleaching, as indicated by the minimal change in the MLCT band (Fig. S44,† inset). We hypothesize that the observed drop after three iterations may be associated with the depletion of Asc-Ac resulting in the slower kinetics due to a constant trigger. To ascertain that oxygen is indeed the predominant factor mediating the process and to rule out the formation of other species such as **Pt-tBu-Asc-Ac**, we conducted experiments upon Ar-purging and visually tracked the re-diffusion of minute oxygen traces into the system. The lifetimes of the Ar-purged samples, both with and without Asc-Ac, were identical (Fig. S48 and S51†). Notably, after irradiating the Ar-purged mixture yet including Asc-Ac, even the last traces of oxygen are evidently scavenged (Fig. 3a, S51 and S52†) while maximizing the lifetime.

Contrastingly, in an open system (*i.e.*, with air headspace), the significant drop of lifetime upon passive oxygen re-equilibration was confirmed by lifetime measurements at different recovery times. Monitoring irradiation of the system in the photoreactor, followed by immediate and delayed (2 min) lifetime measurements, a drastic shortening was observed

(Fig. 3a). This rapid re-equilibration of the system through passive oxygen diffusion (after the quencher has been scavenged) illustrates the dynamic nature of the process. Furthermore, the intensity gradient at the interface can be visually observed under UV light (inset Fig. 3a), confirming that the  $^3\text{O}_2$  is the central actor. To gain further insights into how sustained stress exposure affects the system's resilience, we systematically re-equilibrated the mixture after each irradiation cycle (90 s) with air (Fig. 3b and c).

We observed two significant features: the adaptation ability at each cycle (before complete breakdown) depends on the concentration of both **Pt-tBu** and Asc-Ac. Increasing the concentration of **Pt-tBu** and Asc-Ac leads to a longer stability of the system, which can be explained in two ways: Firstly, higher **Pt-tBu** concentrations generate comparatively more  $^1\text{O}_2$  accompanied by an increased conversion of Asc-Ac before bleaching of **Pt-tBu** can occur. Secondly, the conversion capacity increases with a higher Asc-Ac concentration, thereby hindering the reaction of **Pt-tBu** with  $^1\text{O}_2$ . However, after several cycles, the system undergoes degradation with exhaustion and observable depression due to permanent re-equilibration with the stressor. Mass spectrometry revealed that the photobleaching and the generated  $\text{H}_2\text{O}_2$  results in the formation of a non-emissive Pt(IV) derivative of **Pt-tBu**, wherein oxygen occupies an axial position (Fig. S33†). Overall, the response resembles initial performance boost of biological systems as a response to an aggressor, followed by fatigue and breakdown upon repeated or sustained exposure to harm.<sup>46</sup> Hence, adaptation to stress with suppression of the stressor ( $^3\text{O}_2$ ) causes an overperformance of the system (higher luminescence intensity), much like an organism immediately adapting to stress (adrenaline, short-term response) and coping with it in a sustained manner (cortisol, mid-term response); however, sustained exposure causes fatigue and failure.<sup>47,48</sup>

To ultimately demonstrate the broad applicability of the concept, we subjected different photosensitizing coordination compounds (including **Ir(III)**,<sup>49</sup> **Ru(II)**<sup>50</sup> and **Re(I)**<sup>51</sup> complexes as

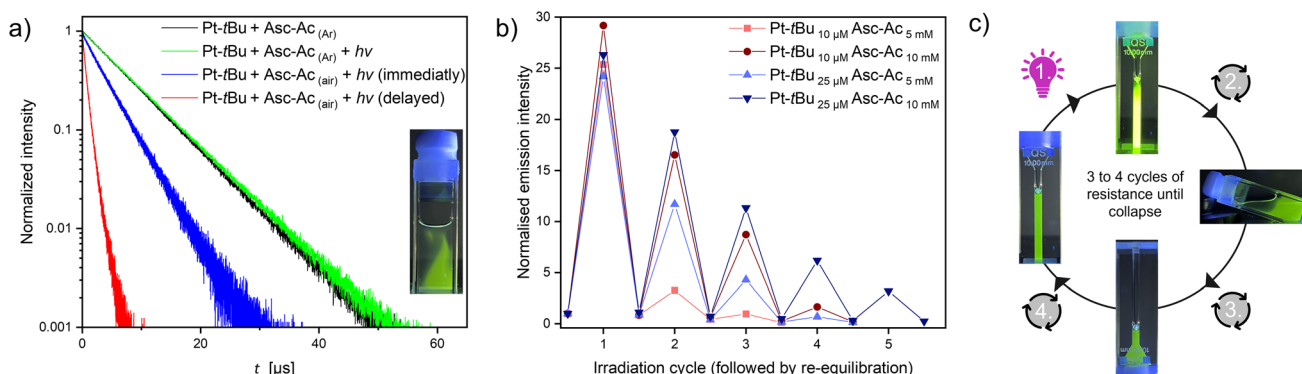


Fig. 3 (a) Immediate (blue) and delayed (red) luminescence lifetime measurement (monitored at 514 nm) of the mixture (**Pt-tBu** 25  $\mu$ M and Asc-Ac 10 mM with an air headspace) after the irradiation process in the photoreactor; comparison with Ar-purged mixtures before (black) and after irradiation (green). Inset: picture of the air-equilibrated cuvette shortly after irradiation under UV light ( $\lambda_{\text{ex}} = 365$  nm). (b) Plot of the emission intensity at 514 nm  $vs.$  the number of irradiation cycles at different concentrations of **Pt-tBu** and Asc-Ac (with air headspace) at room temperature in DMF. Each cycle consists of irradiation in the photoreactor ( $\lambda_{\text{ex}} = 365$  nm) and subsequent re-equilibration with the headspace by shaking the cuvette. The system shows a resistance against stressor replenishment but collapses after multiple re-equilibrations by the formed products. (c) Schematic illustration of an irradiation cycle under UV light ( $\lambda_{\text{ex}} = 365$  nm).



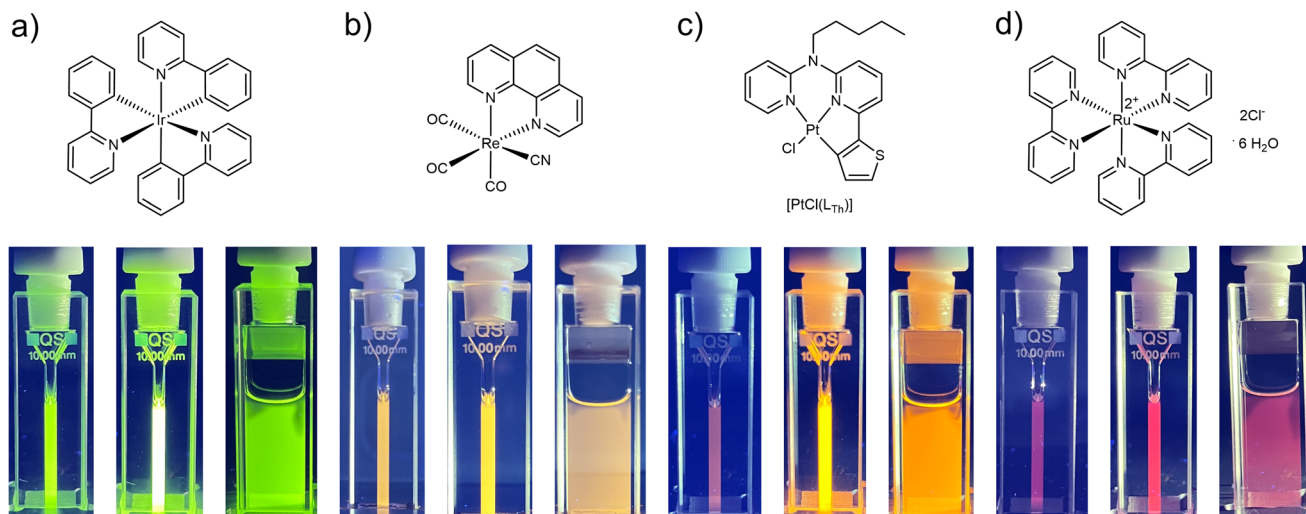


Fig. 4 Structural formulae of *fac*-tris-(2-phenylpyridine)iridium(III)<sup>49</sup> (a), tricarbonyl(cyanido)(1,10-phenanthroline)rhenium(I) (b),<sup>51</sup>  $[\text{PtCl}(\text{L}_{\text{Th}})]^{24}$  (c) and tris(2,2'-bipyridyl)ruthenium(II) dichloride hexahydrate<sup>50</sup> (d). Shown are the corresponding pictures of the cuvettes with each complex (25  $\mu\text{M}$ ) and Asc-Ac (10 mM) in DMF before and after the irradiation in a photoreactor (as observed under UV light,  $\lambda_{\text{ex}} = 365 \text{ nm}$ ). Pictures on the right demonstrate the diffusion of fresh oxygen from the headspace after irradiation.

well as another Pt(II)<sup>24</sup> species, 25  $\mu\text{M}$ ) to irradiation with Asc-Ac (10 mM) in DMF (Fig. 4). Remarkably, Asc-Ac scavenges the photosensitized  $^1\text{O}_2$  generated by the three PS, resulting in a significant increase in emission intensity upon adaptation in the respective emission maxima from green to red (Fig. 4a–c, middle cuvettes). The rapid re-equilibration of the system, driven by passive oxygen diffusion, can be visually observed at the interface (Fig. 4a–c, right cuvettes), which underlines the generality of this adaptation for all tested PS and demonstrates the broad scope of our antioxidative mechanism.

## Conclusion

In conclusion, we have developed a bioinspired strategy based on the use of vitamin C as the antioxidant to adaptively protect molecular phosphors from the long-standing limitation of photodegradation by molecular oxygen. As a proof-of-concept, we have focused on a new Pt(II) complex, and the generality of our approach has been validated by examination of various types of coordination compounds. In air-equilibrated solutions, all luminophores undergo quenching and photobleaching. However, the addition of ascorbic acid with concomitant irradiation deactivates the stressor (molecular oxygen), and restores the phosphorescence. However, repeated exposure to the stressor for over several cycles ultimately surpasses the system's resilience. This demonstrated at chemical level how repeated stress exposure influences a system until it reaches exhaustion. It draws parallels to the immune response, where prolonged triggers can lead to pathological responses, shifting from persistent chronic inflammation to organ failure.<sup>45</sup> Hence, oxidation of the Pt(II) to a new Pt(IV) species mediates the breakdown, much like a dysregulated response in the immune system. Adaptation results from a complex array (here, multi-component mixtures) that is kept out of equilibrium (by irradiation) while involving multiple feedback loops (e.g.,

photosensitization and trapping of singlet dioxygen), followed by degradation of the photosensitizer (in this case, by the accumulation of less reactive peroxides). Our results pave the way for photoluminescence protection and broaden the scope of molecular adaptation<sup>52</sup> to complex multicomponent mixtures.

## Data availability

The data supporting the findings of this study are provided in the ESI† and are available from the corresponding author on request.

## Author contributions

T. R. and C. A. S. designed the project. T. R. performed the synthesis, UV-Vis and photoluminescence studies. T. R. and A. H. conducted all NMR studies. T. R. and S. B. performed the photoirradiation studies. T. R., G. F. and C. A. S. prepared the first draft of the manuscript including the figures, which was then revised and adapted upon contribution from all authors. The overall project was supervised by G. F. and C. A. S.

## Conflicts of interest

The authors declare no competing interests.

## Acknowledgements

T. R., G. F. and C. A. S. gratefully acknowledge funding from the Deutsche Forschungsgemeinschaft (DFG, German Research Foundation) – Collaborative Research Centre (CRC) 1450-431460824 *inSight*. Furthermore, T. R., S. B., G. F. and C. A. S. gratefully acknowledge the CRC 1459-433682494 *Intelligent Matter* (DFG). C. A. S. gratefully acknowledges the generous

financial support for the acquisition of an *Integrated Confocal Luminescence Spectrometer with Spatiotemporal Resolution and Multiphoton Excitation* (DFG/Land NRW: INST 211/915-1 FUGG; DFG EXC1003 *Cells in Motion*: "Berufungsmittel")

## References

- 1 A. Krieger-Liszakay, *J. Exp. Bot.*, 2005, **56**, 337–346.
- 2 D. Njus, P. M. Kelley, Y.-J. Tu and H. B. Schlegel, *Free Radical Biol. Med.*, 2020, **159**, 37–43.
- 3 G. G. Kramarenko, S. G. Hummel, S. M. Martin and G. R. Buettner, *Photochem. Photobiol.*, 2006, **82**, 1634–1637.
- 4 P. Washko, D. Rotrosen and M. Levine, *J. Biol. Chem.*, 1989, **264**, 18996–19002.
- 5 A. C. Carr and S. Maggini, *Nutrients*, 2017, **9**, 1211.
- 6 A. D. Nidhankar, Goudappagouda, P. Kothavade, S. D. Dongre, S. Dnyaneshwar Veer, S. Ranjan Dash, K. Rajeev, K. N. N. Unni, K. Shanmuganathan and S. S. Babu, *Chem.-Asian J.*, 2023, **18**, e202300276.
- 7 A. D. Nidhankar, Goudappagouda, V. C. Wakchaure and S. S. Babu, *Chem. Sci.*, 2021, **12**, 4216–4236.
- 8 A. Sakaya, I. O. L. Bacellar, J. L. Fonseca, A. M. Durantini, J. McCain, L. Xu, M. Vignoni, A. H. Thomas, M. S. Baptista and G. Cosa, *Langmuir*, 2023, **39**, 442–452.
- 9 R. P. Zanocco, R. Bresoli-Obach, F. Nájera, E. Pérez-Inestrosa, A. L. Zanocco, E. Lemp and S. Nonell, *Sensors*, 2023, **23**, 4603.
- 10 M. Mauro, *Chem. Commun.*, 2021, **57**, 5857–5870.
- 11 J. Sanning, L. Stegemann, P. R. Ewen, C. Schwermann, C. G. Daniliuc, D. Zhang, N. Lin, L. Duan, D. Wegner, N. L. Doltsinis, *et al.*, *J. Mater. Chem. C*, 2016, **4**, 2560–2565.
- 12 A. Benosmane, B. Gündüz, M. A. Benaouida, C. Boukentoucha and H. Merzig, *J. Mol. Struct.*, 2023, **1273**, 134254.
- 13 X. Wang, Y. Han, Y. Liu, G. Zou, Z. Gao and F. Wang, *Angew. Chem., Int. Ed.*, 2017, **56**, 12466–12470.
- 14 Q. Wan, D. Li, J. Zou, T. Yan, R. Zhu, K. Xiao, S. Yue, X. Cui, Y. Weng and C.-M. Che, *Angew. Chem., Int. Ed.*, 2022, **61**, e202114323.
- 15 E. Baggaley, I. V. Sazanovich, J. A. G. Williams, J. W. Haycock, S. W. Botchway and J. A. Weinstein, *RSC Adv.*, 2014, **4**, 35003–35008.
- 16 X. Zhen, R. Qu, W. Chen, W. Wu and X. Jiang, *Biomater. Sci.*, 2021, **9**, 285–300.
- 17 A. Colombo, F. Fiorini, D. Septiadi, C. Dragonetti, F. Nisic, A. Valore, D. Roberto, M. Mauro and L. de Cola, *Dalton Trans.*, 2015, **44**, 8478–8487.
- 18 J. Valdes-García, J. Zamora-Moreno, C. Pinzón-Vanegas, A. O. Viviano-Posadas, D. Martínez-Otero, J. Barroso-Flores, B. Ortiz-Lopez, V. F. Ortiz-Navarrete and A. Dorazco-González, *Inorg. Chem.*, 2023, **62**, 6629–6641.
- 19 A. Hagfeldt, G. Boschloo, L. Sun, L. Kloo and H. Pettersson, *Chem. Rev.*, 2010, **110**, 6595.
- 20 C. R. Rao and D. C. Trivedi, *Coord. Chem. Rev.*, 2005, **249**, 613–631.
- 21 W.-Y. Wong, Z. He, S.-K. So, K.-L. Tong and Z. Lin, *Organometallics*, 2005, **24**, 4079–4082.
- 22 P. Hartmann, M. J. Leiner and P. Kohlbacher, *Sens. Actuators, B*, 1998, **51**, 196–202.
- 23 C. Liu, H. Yu, X. Rao, X. Lv, Z. Jin and J. Qiu, *Dyes Pigm.*, 2017, **136**, 641–647.
- 24 S. Buss, L. Geerkens, I. Maisuls, J. Kösters, N. Bäumer, G. Fernández and C. A. Strassert, *Organometallics*, 2024, **43**, 1736–1751.
- 25 T. M. Kirse, I. Maisuls, M. P. Denofrio, A. Hepp, F. M. Cabrerizo and C. A. Strassert, *Organometallics*, 2024, **43**, 1752–1765.
- 26 Z. Li, Y. Han and F. Wang, *Nat. Commun.*, 2019, **10**, 3735.
- 27 B. Li, L. Lin, H. Lin and B. C. Wilson, *J. Biophotonics*, 2016, **9**, 1314–1325.
- 28 W. Wu, X. Shao, J. Zhao and M. Wu, *Adv. Sci.*, 2017, **4**, 1700113.
- 29 T. Theiss, S. Buss, I. Maisuls, R. López-Arteaga, D. Brünink, J. Kösters, A. Hepp, N. L. Doltsinis, E. A. Weiss and C. A. Strassert, *J. Am. Chem. Soc.*, 2023, **145**, 3937–3951.
- 30 D. A. K. Vezzu, J. C. Deaton, J. S. Jones, L. Bartolotti, C. F. Harris, A. P. Marchetti, M. Kondakova, R. D. Pike and S. Huo, *Inorg. Chem.*, 2010, **49**, 5107–5119.
- 31 S. Wilde, D. González-Abadelo, C.-G. Daniliuc, M. Böckmann, N. L. Doltsinis and C. A. Strassert, *Isr. J. Chem.*, 2018, **58**, 932–943.
- 32 S. M. Borisov, G. Nuss and I. Klimant, *Anal. Chem.*, 2008, **80**, 9435–9442.
- 33 S. M. Borisov, R. Saf, R. Fischer and I. Klimant, *Inorg. Chem.*, 2013, **52**, 1206–1216.
- 34 E. F. F. Da Silva, F. M. Pimenta, B. W. Pedersen, F. H. Blaikie, G. N. Bosio, T. Breitenbach, M. Westberg, M. Bregnø, M. Etzerodt, L. G. Arnaut and P. R. Ogilby, *Integr. Biol.*, 2016, **8**, 177–193.
- 35 A. Touthkine, D.-V. Nguyen and K. M. Hahn, *Org. Lett.*, 2007, **9**, 2775–2777.
- 36 A. Cui, X. Peng, J. Fan, X. Chen, Y. Wu and B. Guo, *J. Photochem. Photobiol. A*, 2007, **186**, 85–92.
- 37 Y. Luo, D. Tang, Z. Chen, C. Fu, Z. Xu and J. Meng, *J. Phys. Chem. C*, 2018, **122**, 16872–16878.
- 38 X. Wang, Z. Chai, R. Ma, L. Zhao, Z. Zhang, Y. An and L. Shi, *J. Colloid and Interface Sci.*, 2012, **388**, 80–85.
- 39 J. H. M. van der Velde, J. Oelerich, J. Huang, J. H. Smit, M. Hiermaier, E. Ploetz, A. Herrmann, G. Roelfes and T. Cordes, *J. Phys. Chem. Lett.*, 2014, **5**, 3792–3798.
- 40 J. Wang, S. Zhou, B. Li, X. Liu, H. Chen and H. Wang, *ChemPhotoChem*, 2022, **6**, e202200124.
- 41 G. F. Hassan, N. E. H. Saad, M. Hmadedh and P. Karam, *Dalton Trans.*, 2018, **47**, 15765–15771.
- 42 T. Brandl, C. Kerzig, L. Le Pleux, A. Prescimone, O. S. Wenger and M. Mayor, *Chem.-Eur. J.*, 2020, **26**, 3119.
- 43 S. Buss, M. V. Cappellari, A. Hepp, J. Kösters and C. A. Strassert, *Chemistry*, 2023, **5**, 1243–1255.
- 44 M. E. Gutierrez Suburu, M. Blanke, L. Geerkens, A. Hepp, I. Maisuls, J. Kösters, T. Neumann, J. Voskuhl, M. Giese and C. A. Strassert, *Aggregate*, 2024, e473.
- 45 M. G. Netea, F. Balkwill, M. Chonchol, F. Cominelli, M. Y. Donath, E. J. Giamparellos-Bourboulis, D. Golenbock, *Organometallics*, 2005, **24**, 4079–4082.



M. S. Gresnigt, M. T. Heneka, H. M. Hoffman, *et al.*, *Nat. Immunol.*, 2017, **18**, 826–831.

46 J. Rossaint and A. Zarbock, *Cardiovasc. Res.*, 2015, **107**, 386–395.

47 A.-M. Bao, G. Meynen and D. F. Swaab, *Brain Res. Rev.*, 2008, **57**, 531–553.

48 M. Joëls and T. Z. Baram, *Nat. Rev. Neurosci.*, 2009, **10**, 459–466.

49 S. Lamansky, P. Djurovich, D. Murphy, F. Abdel-Razzaq, R. Kwong, I. Tsyba, M. Bortz, B. Mui, R. Bau and M. E. Thompson, *Inorg. Chem.*, 2001, **40**, 1704–1711.

50 J. A. Broomhead, C. G. Young and P. Hood, *Inorg. Synth.*, 1990, **28**, 338–340.

51 R. M. Leisure, L. A. Sacksteder, D. Nesselrodt, G. A. Reitz, J. N. Demas and B. A. DeGraff, *Inorg. Chem.*, 1991, **30**, 3722–3728.

52 T. Dünnebacke, N. Niemeyer, S. Baumert, S. Hochstädt, L. Borsdorf, M. R. Hansen, J. Neugebauer and G. Fernández, *Nat. Commun.*, 2024, **15**, 5695.

